Geophysical Research Letters

RESEARCH LETTER
10.1029/2020GL090035

Key Points:

- Glacial-interglacial cycles can be incompletely recorded in the ocean due to cancellation of hemispherically antiphased signals
- Precessional cancellation develops due to mixing of North Atlantic and Southern Ocean $\delta^{18}O$ signals at depth
- Model experiments show widespread precessional cancellation for the Early Pleistocene

Supporting Information:

- Supporting Information S1

Correspondence to:
A. L. Morée,
annemoree@gmail.com

Citation:
Morée, A. L., Sun, T., Bretones, A., Straume, E. O., Nisancioglu, K., & Gebbie, G. (2021). Cancellation of the precessional cycle in $\delta^{18}O$ records during the Early Pleistocene. *Geophysical Research Letters*, *48*, e2020GL090035. https://doi.org/10.1029/2020GL090035

Received 4 AUG 2020
Accepted 16 DEC 2020

Cancellation of the Precessional Cycle in $\delta^{18}O$ Records During the Early Pleistocene

Anne L. Morée[1], Tianyi Sun[2,3], Anaïs Bretones[4], Eivind O. Straume[5], Kerim Nisancioglu[4,5], and Geoffrey Gebbie[6]

[1]Geophysical Institute, University of Bergen and the Bjerknes Centre for Climate Research, Bergen, Norway, [2]Institute for Geophysics, Jackson School of Geosciences, The University of Texas at Austin, Austin, TX, USA, [3]Now at Environmental Defense Fund, New York, NY, USA, [4]Department of Earth Science, University of Bergen and the Bjerknes Centre for Climate Research, Bergen, Norway, [5]Centre for Earth Evolution and Dynamics (CEED), Department of Geosciences, University of Oslo, Oslo, Norway, [6]Department of Physical Oceanography, Woods Hole Oceanographic Institution, Woods Hole, MA, USA

Abstract The dominant pacing of glacial-interglacial cycles in deep-ocean $\delta^{18}O$ records changed substantially during the Mid-Pleistocene Transition. The precessional cycle (~23 ky) is absent during the Early Pleistocene, which we show can be explained by cancellation of the hemispherically antiphased precessional cycle in the Early Pleistocene interior ocean. Such cancellation develops due to mixing of North Atlantic and Southern Ocean $\delta^{18}O$ signals at depth, and shows characteristic spatial patterns. We explore the cancellation potential for different North Atlantic and Southern Ocean deep-water source $\delta^{18}O$ values using a tracer transport ocean model. Cancellation of precession occurs for all signal strengths and is widespread for a signal strength typical for the Early Pleistocene. Early Pleistocene precessional power is therefore likely incompletely archived in deep-sea $\delta^{18}O$ records, concealing the true periodicity of the glacial cycles in the two hemispheres.

Plain Language Summary $\delta^{18}O$ records from deep-sea sediments show a pronounced difference in periodicity between the Early (~2-1 Million years ago) and Late (~1-0 Million years ago) Pleistocene—the Mid-Pleistocene Transition (MPT). Representing changes in ice volume and temperature, these $\delta^{18}O$ records are an important source for our understanding of long-term climate variability. A central conclusion based on these $\delta^{18}O$ records is that glacial-interglacial cycles considerably changed their rhythm during the Mid-Pleistocene. Curiously, the ~23,000-year (precessional) cycle of insolation is absent in Early Pleistocene $\delta^{18}O$ records—despite its presence in insolation forcing to the ice sheets. Climate feedbacks involving (sea) ice, geological processes and carbon cycling may have contributed to the MPT. We, however, show that the absence of an Early Pleistocene precession signal in deep-sea $\delta^{18}O$ records could be the result of destructive interference in the deep ocean, caused by the antiphasing of the precessional cycle between the North Atlantic and Southern Ocean deep-water sources. We explore the potential for cancellation with an ocean model and show that interference can indeed cause widespread cancellation, particularly in the Early Pleistocene. We, therefore, conclude that the $\delta^{18}O$ incompletely archives climatic cycles, challenging our understanding of long-term climate variability.

1. Introduction

Changes in the Earth's orbital parameters cause variations in insolation related to the Milankovitch cycles on the time scales of precession (~23 ky), obliquity (~41 ky) and eccentricity (~100 ky) (Milankovic, 1920). In the early 1980s, it became clear that the orbital parameters strongly correlate with the dramatic variations in marine sediment $\delta^{18}O$ records during the Pleistocene (Imbrie et al., 1984). As marine $\delta^{18}O$ relates to ice sheet volume and temperature (Elderfield et al., 2012), Pleistocene glacial-interglacial variations were postulated to be paced by the Milankovitch cycles (Hays et al., 1976; Imbrie et al., 1984). $\delta^{18}O$ proxy records, however, show a pronounced change in dominant Milankovitch periodicities from the Early to Late Pleistocene at the Mid Pleistocene Transition (MPT). The Early Pleistocene (here taken as 2.0–1.2 Ma) is referred to as "the 41 ky world" (Raymo & Nisancioglu, 2003) due to the dominance of the 41 ky obliquity periodicity in the proxy records. The Late Pleistocene (here taken as 0.8–0 Ma) is referred to as "the 100 ky world" because

of the dominance of periodicities between 80 and 120 ky, and has all three Milankovitch cycles represented in deep-sea $\delta^{18}O$ records.

The transition from the 41 ky to the 100 ky world (i.e., the MPT) is not yet fully understood. Most hypotheses explain the MPT by changes in global or hemispheric ice sheet volume, where smaller ice sheets are considered to respond on shorter timescales (i.e., 23 and 41 ky cycles), whereas larger ice sheets respond on longer timescales (i.e., 100 ky cycles). A higher atmospheric pCO_2 is reconstructed for the Early Pleistocene as compared to the Late Pleistocene, particularly for the glacials (Hönisch et al., 2009; Seki et al., 2010). This comparatively high Early Pleistocene atmospheric pCO_2 is associated with smaller ice sheets, while lower atmospheric pCO_2 favors colder climates and larger ice sheets in the Late Pleistocene. The relatively smaller Early Pleistocene ice sheet volume could also be related to the existence and slow erosion of a relatively soft regolith bed beneath the Laurentide ice sheet, inhibiting the build-up of larger ice volume pre-MPT (Clark et al., 2006; Clark & Pollard, 1998). Sea ice may have played a role: the activation of the "sea ice switch" during the MPT due to general Pleistocene climate cooling could have paced a ~100 ky rhythm of the ice ages post-MPT through its influence on atmospheric temperature and moisture fluxes (Gildor & Tziperman, 2000). Alternatively, the change in periodicity could be explained by climate variability on timescales beyond the Pleistocene, where the MPT triggered a different cyclic variability through the albedo discontinuity at the snow-ice edge (Crowley & Hyde, 2008). Recently, however, studies increasingly stress the importance of long-term atmospheric pCO_2 and temperature decline, interacting with regolith removal and/or Southern Ocean iron fertilization as the driver of the MPT (Berger et al., 1999; Chalk et al., 2017; McClymont et al., 2013; Willeit et al., 2019).

2. The Antiphase Hypothesis

An alternative view of both "the 41 ky world" and the MPT is that part of the change in periodicity observed in the $\delta^{18}O$ proxy records is due to the cancellation of the cyclic precessional signals in the interior ocean (Nisancioglu, 2004; Raymo et al., 2006). We build on this work and test the feasibility of cancellation of the hemispherically antiphased precessional signal in deep-sea $\delta^{18}O$ records (the "Antiphase Hypothesis"; Shakun et al., 2016), and note strong spatial variations in the occurrence of such cancellation. According to the Antiphase Hypothesis, precessional cancellation occurs before the MPT only (i.e., in the Early Pleistocene). This contrast in the occurrence of precessional cancellation across the MPT is explained by variations in the relative $\delta^{18}O$ source signal strengths from the two main deep-water formation regions (in the North Atlantic and Southern Ocean)—which influence the strength of precession relative to obliquity at depth. Consequently, the change in source-signal strengths is recorded in the $\delta^{18}O$ of marine sediments as an apparent change in dominant periodicity.

There are several lines of evidence in favor of the Antiphase Hypothesis. For example, one would expect a prominent precessional influence throughout the Pleistocene based on classic Milankovitch theory. In addition, evidence for precession-driven Northern Hemispheric ice volume (Raymo et al., 2006; Shakun et al., 2016) implies a prominent precession component in $\delta^{18}O$ records throughout the Pleistocene. Also, Antarctic and Southern Hemisphere records support the theory that a dynamic Antarctic ice sheet varied in phase with precession from ~3.3 Ma (as recorded off Wilkes Land; Patterson et al., 2014), and contributed with a southern sourced precession signal to the sea level variability (e.g., as evidenced by sea level records off New Zealand; Grant et al., 2019). Under the Antiphase Hypothesis, both of these dynamical expectations would hold, as long as both poles contribute a precession $\delta^{18}O$ signal to the interior ocean. Given new proxy data, we will be able to verify to what extent deep-sea $\delta^{18}O$ indeed represents surface climatic oscillations by using proxies of ice volume not influenced by interior cancellation of precession—such as $\delta^{18}O$ records from Antarctic ice core records across the MPT (Dahl-Jensen, 2018).

The Antiphase Hypothesis (Nisancioglu, 2004; Raymo et al., 2006) argues for a cancellation of the precession signal in global ice volume, and that a benthic stack of $\delta^{18}O$ would record these changes (e.g., Lisiecki & Raymo, 2005). While glacial-interglacial changes bring about a global shift in the water cycle and atmospheric $\delta^{18}O$, the melting of ice sheets imparts a regional signal in seawater $\delta^{18}O$ that is evident in the North Atlantic during the last deglaciation (Waelbroeck et al., 2011). Recent evidence also indicates that the growth of ice sheets occurs via moisture derived from a wide oceanic region but within the same

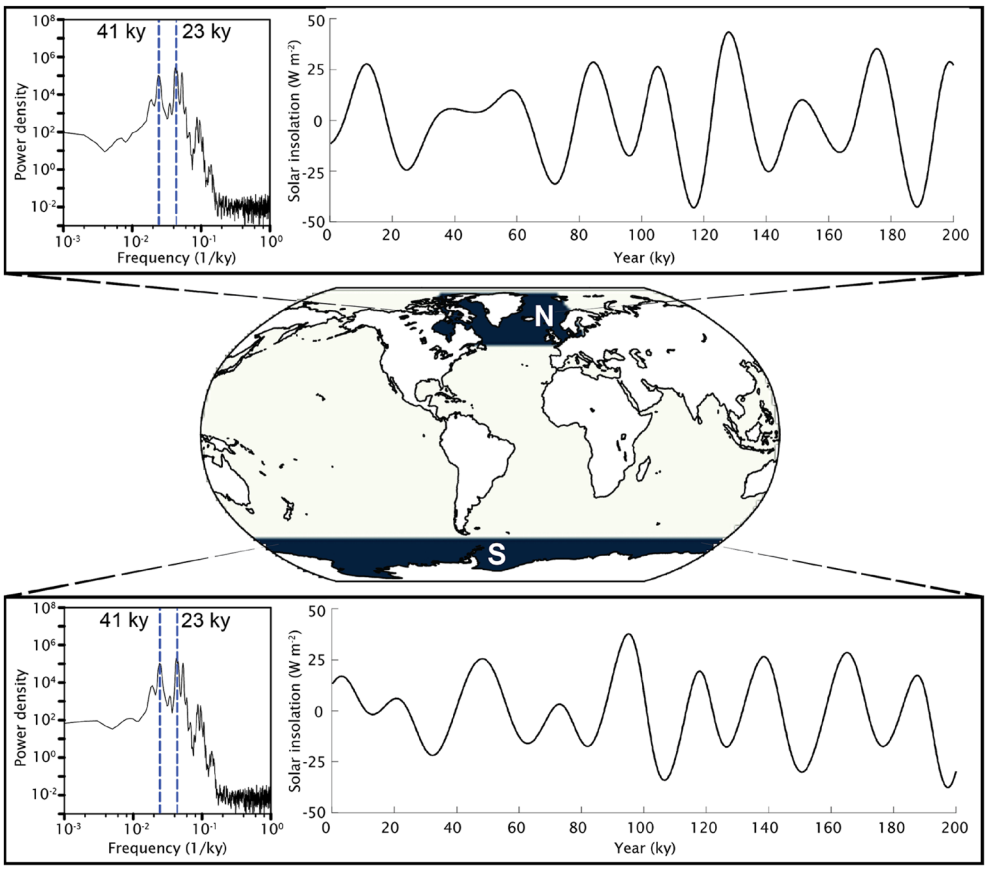

Figure 1. Scaled mean insolation forcing (W m^{-2}) at 65°N (May–July) and 65°S (November–January) with the corresponding power density spectrum (W^2 m^{-4} ky) of the northern (i.e., North Atlantic, within 50–80°N and 100°W–20°E) and southern (i.e., Southern Ocean, south of 60°S) source regions. These two source regions are named N and S on the map.

hemisphere (Rhines & Huybers, 2014), again suggesting that changes in ice sheet volume are reflected in water masses formed in their respective hemispheres. Here we go beyond the original Antiphase Hypothesis to incorporate this new evidence, to investigate how hemispherically asymmetric signals mix in the ocean, and to determine the deep-sea locations where these signals can destructively interfere. Ultimately, we wish to determine whether our hypothesized regional variations can explain the dominance of 41 ky variability in the early Pleistocene benthic $\delta^{18}O$ stack.

3. Methodology

3.1. Model and Experimental Setup

Assuming that deep-water formation mostly occurs during the winter season in both hemispheres, we hypothesize that the mixing of deep-water from the two main deep-water formation regions (the Southern Ocean and North Atlantic; Figure 1) can lead to cancellation of the precessional signal in deep-sea $\delta^{18}O$ sediment records. This is due to the hemispheric antiphasing of the precessional signal in insolation for a given season (Milankovic, 1920), and because of the inflow of meltwater from the ice sheets into the Southern Ocean and North Atlantic deep-water formation regions (Figure 1). Indeed, sediment records of $\delta^{18}O$ archive the influence from northern and southern deep-water sources on glacial-interglacial timescales (e.g., Völpel et al., 2019). Our approach builds on the study by Raymo et al. (2006), who noted the potential for precessional variations in hemispheric ice volumes to cancel out in globally integrated proxies such as ocean $\delta^{18}O$ or sea level, leaving the in-phase obliquity (41,000 years) component of insolation to dominate

the records. In our experimental setup, we go beyond the study by Raymo et al. (2006) by (1) using a 3D model over the idealized model of Imbrie and Imbrie (1980), and (2) exploring the spatial distribution of the potential for precessional cancellation in the ocean interior.

To do this we use a three-dimensional water mass tracer model (Total Matrix Intercomparison, TMI; Gebbie & Huybers, 2012) and investigate the relative impact of hemispheric ice volume derived surface ocean imprints on the recorded signals at deep sea coring sites. The model's North Atlantic and Southern Ocean surface water end-members are imprinted with their respective solar insolation (at 65°N and 65°S) over the past 200 ky (Figure 1) as tracer dye values at each 200 y time step (for details on experiment design, see Text S1). Note that the spectrum of the forcing contains a similar power for the obliquity and precessional cycles. We apply the TMI model to explore the fate of the cyclic northern and southern surface forcing signals in the interior ocean (Text S2). In particular, we assume that it is the signal near deep-water formation sites (Figure 1) that is primarily transferred to the deep ocean. The respective deep-water volume contribution of the northern and southern sources to the interior are kept constant and represent over ~75% of the total bottom water volume in the model (Figure S1).

The importance of boundary conditions for the interior tracer distribution has been explored extensively with the TMI model, including on paleoclimatic time scales (Oppo et al., 2018). However, the deep-water formation sites and overturning rates may have varied over the Pleistocene (Hasenfratz et al., 2019; Kleiven et al., 2003). We evaluate the potential effects of changes in circulation strength (advection and diffusion) on both irregular and orbital timescales and find only minor spatial effects in the results (Text S3 and Figure S5). In addition, we note that deep water temperature may not be perfectly correlated with seawater $\delta^{18}O$ on orbital time scales which makes the signals recorded in the deep ocean sediments more difficult to interpret. Changes in surface hydrological cycling (such as evaporation and therefore the source signal of the ice) and their effects on deep water $\delta^{18}O$ are not explicitly modeled in this study, but are assumed to be related to ice-sheet volume in the respective hemispheres as may be appropriate on millennial and longer timescales. Furthermore, as we explore the relative strength of northern and southern source signals (Section 3.2), any potential differences in absolute $\delta^{18}O$ ice sheet signals are accounted for (Text S4 and Figure S6).

3.2. Variations of Relative Southern Versus Northern Influence

To explore how the relative amplitude of the southern versus northern deep-water signals affects precessional cancellation in $\delta^{18}O$ proxy records, here we introduce the concept of the south-to-north (S/N) ratio. The S/N ratio depends on the interplay between: (i) the respective deep-water volume contribution of the northern and southern sources and their overturning rates; (ii) the $\delta^{18}O$ source signature of the northern and southern ice sheets; and (iii) the amplitude and the variability of the northern and southern ice sheet volumes. In this study, we combine these factors into an aggregate S/N ratio to account for the fact that the TMI model has fixed deep-water volume contributions. We scale the amplitude of the southern source by a factor between 0.125 and 6 to achieve various S/N ratios. Shifts in the S/N ratio can have implications for other water column tracers as well, especially if changes occur in the deep-water volume contributions from the northern and southern source regions (Marinov et al., 2008). Such changes would induce variations in the interior storage of carbon and atmospheric pCO_2 (Marinov et al., 2008; Toggweiler, 1999)—and therefore the greenhouse effect, which again would influence ice sheet volume and temperature.

As we anticipate that the S/N ratio is key for precessional cancellation, we expect a profound change in the S/N ratio during the MPT—causing precessional cancellation in the $\delta^{18}O$ records before the MPT, but not after. Indeed, the influence of the southern and northern hemisphere on global climate variability varied greatly over the past 35 My (De Vleeschouwer et al., 2017), showing potential for large shifts in the S/N ratio. Since deep-sea $\delta^{18}O$ records are strongly correlated with sea level changes (Spratt & Lisiecki, 2016), reconstructions of glacial-interglacial ice sheet volume variability expressed as sea level equivalents (s.l.e.) can be used to understand past changes in the S/N ratio. Before the Early Pleistocene "41 ky world" (i.e., prior to ~2 Ma), we expect a large S/N ratio of greater than six because it precedes the onset of Northern Hemisphere glaciation (Mudelsee & Raymo, 2005). For the Early Pleistocene, a best (but uncertain) estimate of the S/N ratio is in the range of 0.2–0.5; the northern ice sheet contributed ~20–40 m s.l.e. to glacial-interglacial sea level variability (Berger et al., 1999; Willeit et al., 2015). At the same time, total sea level generally varied by

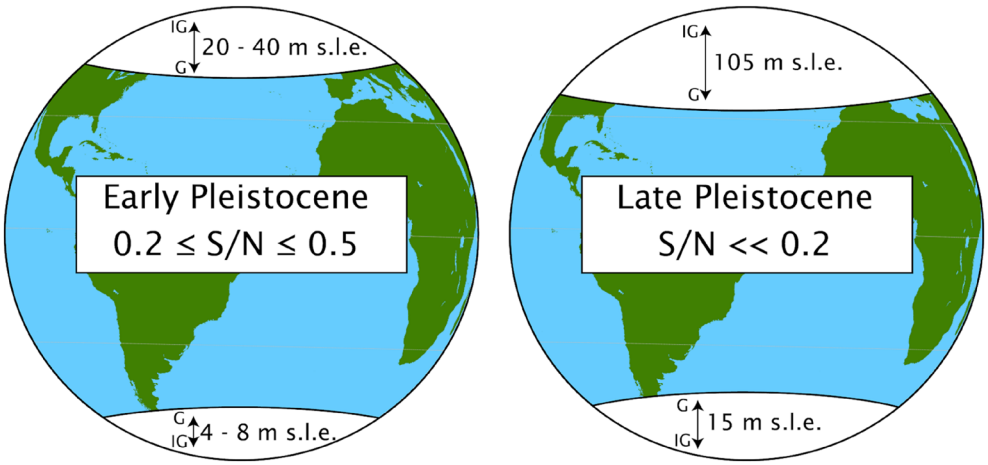

Figure 2. Concept of the decrease in S/N ratio across the MPT from the Early to the Late Pleistocene, as based on s.l.e. reconstructions. The S/N ratio is determined by the relative contribution of the northern versus southern signals (Figure 1). MPT, mid-Pleistocene transition.

at most ~50 m, of which the Antarctic ice sheet contributed 4–8 m s.l.e. (Sutter et al., 2019; Figure 2). After the MPT, global ice sheet volume increased (Berger et al., 1999; Elderfield et al., 2012), with a glacial-interglacial sea level variability reaching ~120 m (Spratt & Lisiecki, 2016). The Antarctic ice sheet likely did not contribute more than ~15 m s.l.e. to glacial-interglacial sea level changes during the Late Pleistocene due to the relative stability of the East Antarctic ice sheet (DeConto & Pollard, 2016; Sutter et al., 2019; Figure 2). Additionally, the transition of the East Antarctic ice sheet from land-based to marine-based during the MPT (Raymo et al., 2006) may have contributed to a decrease in the S/N ratio as the southern ice sheet became in phase with the northern ice sheets.

4. Results

4.1. Cancellation of Precession

Cancellation, or weakening, of the precessional amplitude relative to obliquity amplitude occurs in the ocean interior for any nonzero S/N ratio (Figure 3 and Figure S2), suggesting that such cancellation could occur at any point in Earth's history where deep waters from the two hemispheres (with an antiphased signature) mix in the interior ocean. Our estimate of the Pleistocene S/N ratio is less than 0.5 based on sea level reconstructions (Figure 2). For the Early Pleistocene, the estimated S/N ratio of ~0.2–0.5 indicates that cancellation of precession may have played a major role in $\delta^{18}O$ records, particularly at depth in the Pacific basin (Figure 3 and Figure S2). In the Late Pleistocene, S/N decreased to values <<0.2 for which we do not expect widespread cancellation (Figure 3 and Figure S2), giving an explanation for the reappearance of precession in the post-MPT $\delta^{18}O$ records.

A stronger amplitude of the southern sourced signal (i.e., high S/N ratio) generally pushes the region of cancellation northward in all ocean basins (Figure S2). At the same time, the spatial extent of the bottom water cancellation is greatly reduced when it migrates from the Pacific into the Atlantic basin. The dominant contribution of the southern source waters in the Pacific (Gebbie, 2012; Figure S1) results in widespread Pacific cancellation only when the amplitude of the southern source is relatively weak (S/N < 1). For high S/N ratios (S/N > 6, as expected before the onset of glaciation in the Northern Hemisphere), precessional cancellation is limited to the mid-Atlantic interior ocean (Figure 3). Also for an S/N ratio of ~1–2, we expect no cancellation of precession in the Pacific and very limited cancellation in the Atlantic and Indian Oceans (Figure S2). The amplitude of the southern source signal relative to the northern deep-water source is therefore key in the development of cancellation. An improved estimate of end-member values (i.e., $\delta^{18}O$ from ice released into the ocean) for the Early and Late Pleistocene would help to determine the importance of cancellation for each of these distinct periods.

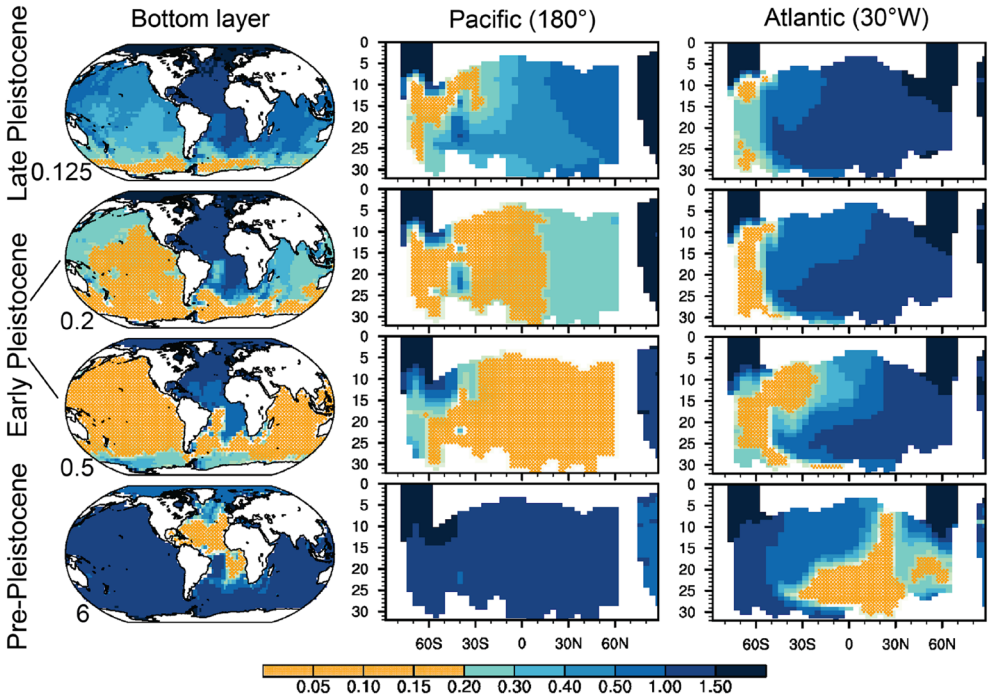

Figure 3. Ratio of precessional to obliquity spectral power, as received from the northern and southern sources (Figure 1). Data are normalized by the 41 ky obliquity power at each grid point (Text S1) and presented for the S/N ratios 0.125, 0.2, 0.5, and 6 as denoted to the lower left of the respective maps. The area where the spectral power is less than 0.2 is hatched (in orange) to show the potential extent of cancellation of precessional power relative to obliquity. White regions received no signal from either the northern or southern sources. Data are presented at the bottom layer, an Atlantic section (at 30°W) and a Pacific section (at 180°). The vertical axis of the sections is in hundreds of meters. The full range of S/N experiments are presented in Figure S2 (bottom layer), Figure S3 (Atlantic), and Figure S4 (Pacific).

There is a notable exception to the dominance of southern source waters in the mid- and high-latitude North Atlantic. Here, the >75% contribution of northern source waters dominates the interior signal and prevents cancellation of the precessional signal relative to obliquity north of ~40°N under the assumption of a modern-day circulation (Figure 3). Our numerical results suggest a more general rule that cancellation requires the product of the S/N ratio and the ratio of North Atlantic Deep Water (NADW) to Antarctic Bottom Water (AABW) water masses to be close to one. Both of these quantities are uncertain for the early Pleistocene. Here, we keep this water-mass ratio at the modern day level and vary the S/N forcing ratio. If the influence of a southern source water-mass was much larger than today in the early Pleistocene, for example, with a weaker influence of NADW and/or stronger influence of AABW, cancellation would be possible also in the mid- and high-latitude North Atlantic. Interestingly, a weak precessional amplitude off the southwestern African coast is present for nearly any S/N ratio (Figure S2). The area prone to cancellation of precession has a vertical structure (Figure 3 and Figures S3 and S4). This shows that most of the interior ocean is prone to cancellation, or weakening of the precessional signal relative to obliquity, but that the cancellation is not spatially uniform.

We conclude that in the South Atlantic, Indian and Pacific Ocean basins, the Early Pleistocene absence of a strong precessional power in $\delta^{18}O$ records could be explained by the mixing of North Atlantic and Southern Ocean sourced deep-water masses. Moreover, this result is robust with respect to changes in circulation strength (Text S3 and Figure S5). If the S/N ratio decreased during the Pleistocene, as suggested by reconstructions of ice sheet volume variability, such cancellation would disappear in the Late Pleistocene—explaining the appearance of a precessional component in deep-sea δ18O records as observed across the Mid Pleistocene Transition.

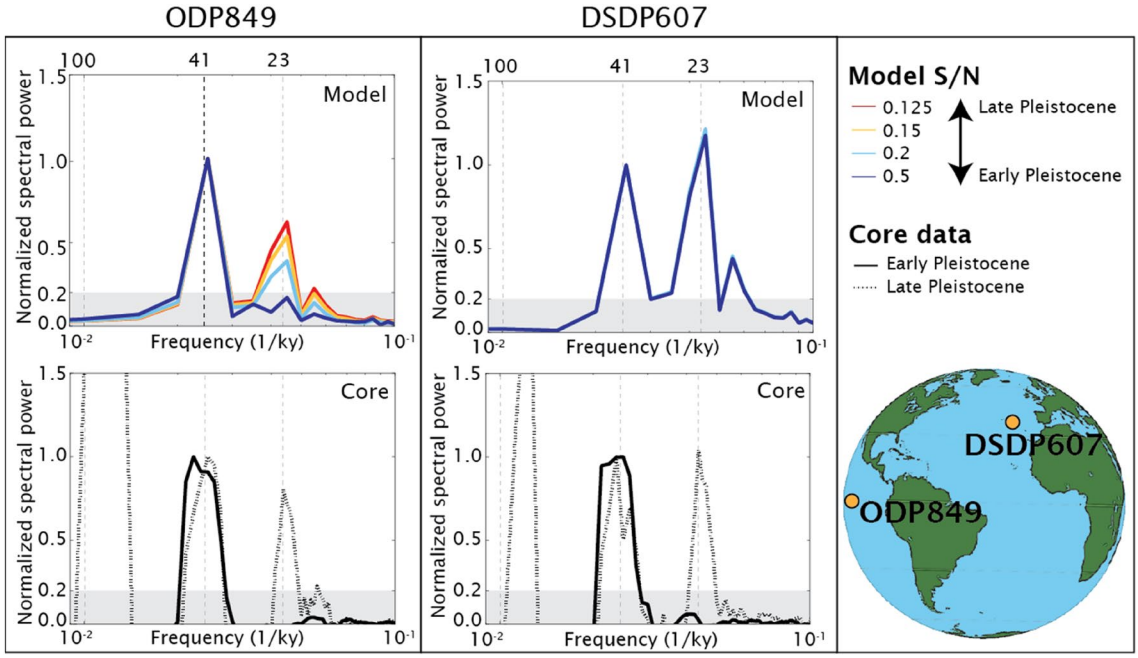

Figure 4. Power spectrum of the model sensitivity experiments and sediment core $\delta^{18}O$ data at core sites ODP849 and DSDP607, after Figure S1 in Raymo et al. (2006). Cancellation is defined at a normalized precessional power <0.2, and is indicated by the gray area. Spectral noise is subtracted from the sediment core data in order to reveal the dominant frequencies (Text S5).

4.2. Comparison of Artificial and Real Sediment Cores

To test the model results of spatially varying cancellation, we analyze the power spectra of deep-sea sediment core ODP849 (mid-Pacific) and DSDP607 (North Atlantic) with depth-derived age-models (Huybers, 2007) and artificial modeled sediment cores taken at the same locations (Figure 4). The artificial sediment cores show the asymmetry in basin response to different S/N ratios. The mid-Pacific core shows cancellation for S/N ratios 0.375 and 0.5. In contrast, the North Atlantic core shows that cancellation is not strong enough to explain the lack of a precessional signal when considering the Pleistocene range of S/N ratios. This asymmetry is a direct consequence of the circulation and water mass contributions in the model, with the Pacific dominated by southern source waters and the North Atlantic dominated by northern source waters, especially north of 30N where core DSDP607 is located (Figure S1). Cancellation is more sensitive to differences in source signal strengths (Figure 3) than to changes in circulation rate (Figure S5)—highlighting that changes in S/N ratio are decisive for the cancellation at a particular core location.

The real sediment cores, on the other hand, show the absence of precessional power at both sites during the Early Pleistocene (Figure 4). This result indicates that cancellation of precession could have played a major role in the interior Pacific during the Early Pleistocene ($0.2 \leq S/N \leq 0.5$, Figure 3 and Figure S2). However, the absence of precessional power at the North Atlantic site appears to be at odds with the model results, given that the simulated North Atlantic and mid-Pacific $\delta^{18}O$ time series respond differently to a change in S/N ratio. This inconsistency could be explained by east-west asymmetries in water-mass distribution across the mid-Atlantic ridge, or by potential circulation changes in the early Pleistocene. For instance, the North Atlantic can exhibit cancellation if the influence of southern source waters increased (Figure S2). Such an increased southern influence could develop through shoaling of the upper Atlantic overturning cell—increasing the volume contribution of the southern source waters to the North Atlantic. Shoaling and northward extension of southern source waters is indeed reconstructed for cold periods during the Pleistocene (Böhm et al., 2014). Another important factor is the potential for changes in the relative strength of the precession and obliquity signal in the two end-members. As postulated by (Raymo et al., 2006), the Antarctic ice sheet transitioned from a largely land-based ice sheet to a marine-based ice sheet at the MPT. This is not only expected to have changed the amplitude of the Southern Hemisphere signal, but also the relative strength of obliquity and precession. Typically, marine based ice sheets are expected to respond less

to precession given that the relative contribution from seasonal surface melt is reduced. Thus, the absence of a pronounced precessional power in Early Pleistocene deep sea $\delta^{18}O$ records may reflect a combination of multiple causes, and resolving the changes in the glacial cycles at the MPT relies on careful consideration of the location and depth of the marine sediment cores.

5. Conclusion and Discussion

Our modeling results show that the cancellation of the precessional signal in deep sea marine sediment records, as expected from the Antiphase Hypothesis, may have played a major role during the Early Pleistocene in the interior of the Pacific Ocean ($0.2 \leq S/N \leq 0.5$, Figure 3, Figure S2, and Figure 4). The cancellation of precession causes an incomplete recording of hemispheric antiphased glacial-interglacial cycles in the deep-sea $\delta^{18}O$ records. We also show that the localities where the cancellation is evident varies with different S/N ratios, representing different contributions from northern and southern deep water, ice volume variability, and $\delta^{18}O$ signatures of the ice sheets.

The basin asymmetry reveals a possible challenge with the interpretation of global stacks of $\delta^{18}O$ records: if interpreted as a whole (Lisiecki & Raymo, 2005), any interbasin asymmetries in spectral power sensitivity to changes in S/N ratio are not considered. Unfortunately, the number of sediment cores available today is not sufficient to test the spatial variation of the cancellation suggested by the model: only five sediment cores meet the two critical requirements of resolving the Early Pleistocene and not being orbitally tuned. Moreover, these five cores are concentrated in only two regions: the tropical East Pacific (e.g., ODP849) and the North Atlantic (e.g., DSDP607). The spectra of the $\delta^{18}O$ time series from the ODP849 and DSDP607 sediment cores both show the absence of precessional power in the Early Pleistocene (Figure 4 and Text S5). This is matched by the simulated power spectra for the tropical East Pacific. However, in the simulated power spectra for the North Atlantic site, the precessional signal is strong for all the S/N ratios investigated, indicating that the deep sea site is dominated by northern sourced water in the model. While the potential for precessional cancellation is widespread in the global ocean, our analysis emphasizes that better constraints on the ocean circulation and water-mass ratio are necessary to quantify precessional cancellation at individual core sites.

Acknowledgments
The authors acknowledge P. Huybers and M. Raymo for discussions that helped improve this manuscript. Insightful comments from two reviewers also helped improve this manuscript. A. L. Morée, T. Sun, A. Bretones, and E. O. Straume thank the organization of Advanced Climate Dynamics Course (ACDC) for creating a nurturing and inspiring environment. This work developed from the ACDC2018 summer school and by funding of T. Sun and E. O. Straume to visit Bergen through their Bjerknes Visiting Fellowship. A. L. Morée thanks the University of Bergen for her stipend, E. O. Straume acknowledges support from the Research Council of Norway through its Centers of Excellence funding scheme (project 223272). T. Sun was supported by the Ewing-Worzel Fellowship at Institute for Geophysics, University of Texas at Austin. Storage and computing resources were provided by UNINETT Sigma2—the National Infrastructure for High Performance Computing and Data Storage in Norway (project number ns2980k). G. Gebbie is supported by the U.S. National Science Foundation award OCE-1536380. Last, the authors thank the DIKU project (number 812957; ACER (Advanced Climate Education and Research) for its support.

Data Availability Statement

The model experiment data are publicly accessible in NetCDF format at the NIRD Research Data Archive at https://doi.org/10.11582/2021.00001 (Morée et al., 2021). The TMI model used in this study is documented in Gebbie & Huybers (2012).

References

Berger, A., Li, X. S., & Loutre, M. F. (1999). Modelling northern hemisphere ice volume over the last 3Ma. *Quaternary Science Reviews*, *18*(1), 1–11. http://www.sciencedirect.com/science/article/pii/S027737919800033X

Böhm, E., Lippold, J., Gutjahr, M., Frank, M., Blaser, P., Antz, B., et al. (2014). Strong and deep Atlantic meridional overturning circulation during the last glacial cycle. *Nature*, *517*, 73. https://doi.org/10.1038/nature14059

Chalk, T. B., Hain, M. P., Foster, G. L., Rohling, E. J., Sexton, P. F., Badger, M. P. S., et al. (2017). Causes of ice age intensification across the Mid-Pleistocene Transition. *Proceedings of the National Academy of Sciences*, *114*, 13114–13119.

Clark, P. U., Archer, D., Pollard, D., Blum, J. D., Rial, J. A., Brovkin, V., et al. (2006). The middle Pleistocene transition: characteristics, mechanisms, and implications for long-term changes in atmospheric pCO2. *Quaternary Science Reviews*, *25*(23), 3150–3184. http://www.sciencedirect.com/science/article/pii/S0277379106002332

Clark, P. U., & Pollard, D. (1998). Origin of the Middle Pleistocene Transition by ice sheet erosion of regolith. *Paleoceanography*, *13*(1), 1–9. https://agupubs.onlinelibrary.wiley.com/doi/abs/10.1029/97PA02660

Crowley, T. J., & Hyde, W. T. (2008). Transient nature of late Pleistocene climate variability. *Nature*, *456*, 226. https://doi.org/10.1038/nature07365

Dahl-Jensen, D. (2018). Drilling for the oldest ice. *Nature Geoscience*, *11*(10), 703–704. https://doi.org/10.1038/s41561-018-0241-2

De Vleeschouwer, D., Vahlenkamp, M., Crucifix, M., & Pälike, H. (2017). Alternating Southern and Northern Hemisphere climate response to astronomical forcing during the past 35 m. y. *Geology*, *45*(4), 375–378. https://doi.org/10.1130/G38663.1

DeConto, R. M., & Pollard, D. (2016). Contribution of Antarctica to past and future sea-level rise. *Nature*, *531*, 591. https://doi.org/10.1038/nature17145

Elderfield, H., Ferretti, P., Greaves, M., Crowhurst, S., McCave, I. N., Hodell, D., & Piotrowski, A. M. (2012). Evolution of ocean temperature and ice volume through the mid-Pleistocene climate transition. *Science*, *337*, 704–709.

Gebbie, G. (2012). Tracer transport timescales and the observed Atlantic-Pacific lag in the timing of the Last Termination. *Paleoceanography*, *27*(3), PA3225. https://doi.org/10.1029/2011pa002273

Gebbie, G., & Huybers, P. (2012). The mean age of ocean waters inferred from radiocarbon observations: Sensitivity to surface sources and accounting for mixing histories. *Journal of Physical Oceanography*, *42*(2), 291–305. https://journals.ametsoc.org/doi/abs/10.1175/JPO-D-11-043.1

Gildor, H., & Tziperman, E. (2000). Sea ice as the glacial cycles' Climate switch: role of seasonal and orbital forcing. *Paleoceanography*, *15*(6), 605–615. https://agupubs.onlinelibrary.wiley.com/doi/abs/10.1029/1999PA000461

Grant, G. R., Naish, T. R., Dunbar, G. B., Stocchi, P., Kominz, M. A., Kamp, P. J. J., et al. (2019). The amplitude and origin of sea-level variability during the Pliocene epoch. *Nature*, *574*(7777), 237–241. https://doi.org/10.1038/s41586-019-1619-z

Hasenfratz, A. P., Jaccard, S. L., Martínez-García, A., Sigman, D. M., Hodell, D. A., Vance, D., et al. (2019). The residence time of Southern Ocean surface waters and the 100,000-year ice age cycle. *Science*, *363*, 1080–1084.

Hays, J. D., Imbrie, J., & Shackleton, N. J. (1976). Variations in the Earth's Orbit: Pacemaker of the Ice Ages. *Science*, *194*(4270), 1121. http://science.sciencemag.org/content/194/4270/1121.abstract

Hönisch, B., Hemming, N. G., Archer, D., Siddall, M., & McManus, J. F. (2009). Atmospheric carbon dioxide concentration across the mid-Pleistocene transition. *Science*, *324*, 1551–1554.

Huybers, P. (2007). Glacial variability over the last two million years: An extended depth-derived agemodel, continuous obliquity pacing, and the Pleistocene progression. *Quaternary Science Reviews*, *26*(1-2), 37–55.

Imbrie, J., Hays, J. D., Martinson, D. G., McIntyre, A., Mix, A. C., Morley, J. J., et al. (1984). The orbital theory of Pleistocene climate: support from a revised chronology of the marine d18O record. In A. Berger, J. Imbrie, J. Hays, G. Kukla, & B. Saltzman (Eds.), *Milankovitch and Climate, Part 1* (pp. 269–305). Dordrecht, The Netherlands: D. Reidel Publishing Company.

Imbrie, J., & Imbrie, J. Z. (1980). Modeling the Climatic Response to Orbital Variations. *Science*, *207*(4434), 943. http://science.sciencemag.org/content/207/4434/943.abstract

Kleiven, H. F., Jansen, E., Curry, W. B., Hodell, D. A., & Venz, K. (2003). Atlantic Ocean thermohaline circulation changes on orbital to suborbital timescales during the mid-Pleistocene. *Paleoceanography*, *18*(1), 8-1–8-13. https://doi.org/10.1029/2001PA000629

Lisiecki, L. E., & Raymo, M. E. (2005). A Pliocene-Pleistocene stack of 57 globally distributed benthic δ18O records. *Paleoceanography*, *20*(1), PA1003. https://agupubs.onlinelibrary.wiley.com/doi/abs/10.1029/2004PA001071

Marinov, I., Gnanadesikan, A., Sarmiento, J. L., Toggweiler, J. R., Follows, M., & Mignone, B. K. (2008). Impact of oceanic circulation on biological carbon storage in the ocean and atmospheric pCO2. *Global Biogeochemical Cycles*, *22*(3), GB3007. http://dx.doi.org/10.1029/2007GB002958

McClymont, E. L., Sosdian, S. M., Rosell-Melé, A., & Rosenthal, Y. (2013). Pleistocene sea-surface temperature evolution: Early cooling, delayed glacial intensification, and implications for the mid-Pleistocene climate transition. *Earth-Science Reviews*, *123*, 173–193. http://www.sciencedirect.com/science/article/pii/S0012825213000809

Milankovic, M. (1920). *Théorie mathématique des phénomènes thermiques produits par la radiation solaire*. Paris: Gauthier-Villars et Cie.

Morée, A. L., Sun, T., Bretones, A., Straume, E., Nisancioglu, K., & Gebbie, G. (2021). Ocean output of TMI model Pleistocene Milankovitch cycle experiments [Data set]. Norstore. https://doi.org/10.11582/2021.00001

Mudelsee, M., & Raymo, M. E. (2005). Slow dynamics of the Northern Hemisphere glaciation. *Paleoceanography*, *20*(4), PA4022. https://doi.org/10.1029/2005PA001153

Nisancioglu, K. H. (2004). Modeling the impact of atmospheric moisture transport on global ice volume. (Ph.D.). *Massachusetts Institute of Technology*. Retrieved from http://hdl.handle.net/1721.1/16703

Oppo, D. W., Gebbie, G., Huang, K.-F., Curry, W. B., Marchitto, T. M., & Pietro, K. R. (2018). Data Constraints on Glacial Atlantic Water Mass Geometry and Properties. *Paleoceanography and Paleoclimatology*, *33*(9), 1013–1034. https://doi.org/10.1029/2018PA003408

Patterson, M. O., McKay, R., Naish, T., Escutia, C., Jimenez-Espejo, F. J., Raymo, M. E., et al. (2014). Orbital forcing of the East Antarctic ice sheet during the Pliocene and Early Pleistocene. *Nature Geoscience*, *7*(11), 841–847. https://doi.org/10.1038/ngeo2273

Raymo, M. E., Lisiecki, L. E., & Nisancioglu, K. H. (2006). Plio-Pleistocene Ice Volume, Antarctic Climate, and the Global $\delta^{18}O$ Record. *Science*, *313*(5786), 492–495.

Raymo, M. E., & Nisancioglu, K. H. (2003). The 41 kyr world: Milankovitch's other unsolved mystery. *Paleoceanography*, *18*(1).

Rhines, A., & Huybers, P. J. (2014). Sea ice and dynamical controls on preindustrial and last glacial maximum accumulation in central Greenland. *Journal of Climate*, *27*(23), 8902–8917. https://doi.org/10.1175/JCLI-D-14-00075.1

Seki, O., Foster, G. L., Schmidt, D. N., Mackensen, A., Kawamura, K., & Pancost, R. D. (2010). Alkenone and boron-based Pliocene pCO2 records. *Earth and Planetary Science Letters*, *292*(1), 201–211. http://www.sciencedirect.com/science/article/pii/S0012821X10000816

Shakun, J. D., Raymo, M. E., & Lea, D. W. (2016). An early Pleistocene Mg/Ca-$\delta^{18}O$ record from the Gulf of Mexico: Evaluating ice sheet size and pacing in the 41-kyr world. *Paleoceanography*, *31*(7), 1011–1027.

Spratt, R. M., & Lisiecki, L. E. (2016). A Late Pleistocene sea level stack. *Climate of the Past*, *12*(4), 1079–1092. https://www.clim-past.net/12/1079/2016/

Sutter, J., Fischer, H., Grosfeld, K., Karlsson, N. B., Kleiner, T., Van Liefferinge, B., & Eisen, O. (2019). Modelling the Antarctic Ice Sheet across the Mid Pleistocene Transition - Implications for Oldest Ice. *The Cryosphere*, *13*(7), 2023–2041.

Toggweiler, J. R. (1999). Variation of atmospheric CO2 by ventilation of the ocean's deepest water. *Paleoceanography*, *14*(5), 571–588. https://doi.org/10.1029/1999PA900033

Völpel, R., Mulitza, S., Paul, A., Lynch-Stieglitz, J., & Schulz, M. (2019). Water mass versus sea level effects on benthic foraminiferal oxygen isotope ratios in the Atlantic Ocean during the LGM. *Paleoceanography and Paleoclimatology*, *34*, 98–121. https://doi.org/10.1029/2018PA003359

Waelbroeck, C., Skinner, L. C., Labeyrie, L., Duplessy, J. C., Michel, E., Vazquez Riveiros, N., et al. (2011). The timing of deglacial circulation changes in the Atlantic. *Paleoceanography*, *26*(3), PA3213. https://doi.org/10.1029/2010PA002007

Willeit, M., Ganopolski, A., Calov, R., & Brovkin, V. (2019). Mid-Pleistocene transition in glacial cycles explained by declining CO2and regolith removal. *Science Advances*, *5*(4), eaav7337. https://doi.org/10.1126/sciadv.aav7337

Willeit, M., Ganopolski, A., Calov, R., Robinson, A., & Maslin, M. (2015). The role of CO2 decline for the onset of Northern Hemisphere glaciation. *Quaternary Science Reviews*, *119*, 22–34. http://www.sciencedirect.com/science/article/pii/S0277379115001572

References From the Supporting Information

Berger, A., & Loutre, M. (1992). Astronomical Solutions for Paleoclimate Studies over the Last 3 Million Years. *Earth and Planetary Science Letters*, *111*(2-4), 369–382.

Gebbie, G., & Huybers, P. (2011). How is the ocean filled?. *Geophysical Research Letters*, *38*(6), L06604. https://doi.org/10.1029/2011gl046769

Gouretski, V., & Koltermann, K. (2004). *WOCE global hydrographic climatology*. Hamburg, Germany.
Huybers, P. (2018). *Matlab code to calculate Milankovitch insolation cycles, modified from J. Levine (2001)*. USA: UC Berkeley and Harvard.
Key, R. M., Kozyr, A., Sabine, C. L., Lee, K., Wanninkhof, R., Bullister, J. L., et al. (2004). A global ocean carbon climatology: Results from Global Data Analysis Project (GLODAP), *Global Biogeochemical Cycles*, *18*(4), GB4031. http://dx.doi.org/10.1029/2004GB002247
Legrande, A. N., & Schmidt, G. A. (2006). Global gridded data set of the oxygen isotopic composition in seawater. *Geophysical Research Letters*, *33*(12), L12604. https://doi.org/10.1029/2006GL026011
Vaughan, S., Bailey, R. J., & Smith, D. G. (2011). Detecting cycles in stratigraphic data: Spectral analysis in the presence of red noise. *Paleoceanography*, *26*(4), PA4211. https://doi.org/10.1029/2011pa002195